Vietnam Journal of Mechanics, Vol. 46, No. 1 (2024), pp. 67 – 79
DOI: https://doi.org/10.15625/0866-7136/20638

ANALYZING THE NONLINEAR TORSIONAL BUCKLING AND POST-BUCKLING OF ES - FG POROUS CYLINDRICAL SHELLS IN THERMAL ENVIRONMENT USING FSDT IN TERMS OF THE DISPLACEMENT COMPONENTS

Pham Van Hoan[1,2,*], **Dao Nhu Mai**[2,3], **Phan Van Ba**[1] **and Le Kha Hoa**[1]
[1]*Military Academy of Logistics, Hanoi, Vietnam*
[2]*Graduate University of Sciences and Technology, VAST, Hanoi, Vietnam*
[3]*Institute of Mechanics, VAST, Hanoi, Vietnam*
[4]*VNU University of Engineering and Technology, Hanoi, Vietnam*
[*]E-mail: lhoanhd@gmail.com

Received: 29 January 2024 / Revised: 21 March 2024 / Accepted: 25 March 2024
Published online: 31 March 2024

Abstract. The main aim of this paper is to investigate the nonlinear buckling and post-buckling of eccentrically stiffened sandwich functionally graded porous (FGP) cylindrical shells surrounded by elastic foundations in thermal environments and under torsional load by analytical approach in terms of the displacement components. The shells are reinforced by eccentric rings and stringers attached to the inside and material properties of face sheets and stiffeners are assumed to be continuously graded in the thickness direction. The sandwich cylindrical shell is composed of FG porous core and two FG layer coating. Based on the first order shear deformation theory (FSDT) with von Kármán geometrical nonlinearity and smeared stiffeners technique, the governing equations are derived. Using Galerkin method, the closed form to find critical torsional load and post-buckling load-deflection curves are obtained. The effects of porosity parameters, the thickness of the porous core, temperature, stiffener, foundation, material and dimensional parameters are analyzed.

Keywords: torsion, FSDT, buckling, post-buckling, ES-FG porous cylindrical shells.

1. INTRODUCTION

Cylindrical shells are used as common structural load-bearing components in modern engineering. Basing on the higher order shear deformation theory, Shen [1] studied

the stability problem of torsion-loaded functionally graded shells in thermal environments. Using the nonlinear large deflection shell theory and Ritz method, Huang and Han [2] researched the nonlinear buckling of unstiffened FGM cylindrical shells. The nonlinear buckling shape observed in the experiment was taken into account in their work. Torsional buckling of elastic cylinders with a hard surface coating layer is studied by Zhang and Fu [3] in which deformations of the core and surface layer are obtained analytically though the Navier's equation and thin shell model. Batra [4] studied the torsion of cylinders with material modulii varying only in the axial direction.

For the stiffened FG cylindrical shell, the stability problem is also very interest subject. Basing on the classical shell theory and FSDT with smeared stiffeners technique, Dung and Hoa [5, 6] studied the nonlinear buckling and post-buckling of functionally graded stiffened thin circular cylindrical shells under torsional load and surrounded by Pasternak elastic foundations. Shells are reinforced by stringers and closely spaced rings in which material properties of the shell and the stiffeners are assumed to be continuously graded in the thickness direction. Using the classical shell theory, Thang et al. [7] investigated the thermomechanical buckling and postbuckling behaviors of a cylindrical shell with functionally graded coatings. The layers of coatings are assumed to be made of functionally graded materials and the core of the shell is made of homogeneous material and the shell is reinforced by outside stringers. With the three-term approximate solution of deflection, Ninh and Bich [8] presented the nonlinear torsional buckling and postbuckling of ceramic functionally graded material eccentrically stiffened cylindrical shell surrounded by Pasternak foundation in thermal environment. The cylindrical shell is reinforced by stringer and ring stiffeners system in which the material properties of shell are continuously graded in the thickness direction.

Recently, Porous materials such as metal foams are an important category of lightweight materials with excellent energy-absorbing capability. Therefore, this type of material has received wide application in practice for structures and the stability problem of these structures is a very interesting subject. There is some research about porous cylindrical shells. Using classical shell theory and analytical method, Nam et al. [9] investigated the nonlinear buckling and post-buckling of FGP circular cylindrical shells reinforced by orthogonal stiffeners surrounded by elastic medium under torsional load in thermal environment. Utilizing the Galerkin method and the fourth-order Runge–Kutta method, Foroutan et al. [10–12] presented the analytical and semi-analytical approaches for the nonlinear dynamic and static hygrothermal buckling analysis of imperfect functionally graded porous cylindrical shells under hygrothermal loading and axial compression. Based on the first-order shear deformation theory, Shahgholian et al. [13, 14] used the Rayleigh-Ritz method to study buckling analyses of functionally graded porous

nanocomposite cylindrical shells reinforced with graphene platelets under uniform external lateral pressure and axially compressive load.

A review of the literature shows that few studies have been done on buckling and post-buckling of FGP cylindrical shells under torsional load in the framework of the shear deformationn theory. The research objective of this paper is to study nonlinear torsional buckling and post-buckling of the stiffened FGP cylindrical shells. The sandwich cylindrical shell is composed of FG porous core and FG face sheets reinforced by FGM stiffeners under torsional load. The material properties of the face sheets and stiffeners are assumed to be continuously graded in the thickness direction according to a simple power-law distribution in terms of volume fraction of constituents. The core layer is made of a porous material (metal foam) characterized by a porosity coefficient. The material continuity of face sheets-core and face sheets-stiffeners is guaranteed. The first-order shear deformation theory and the improved Lekhnitskii's smeared stiffeners technique in conjunction with the Galerkin method are applied to solve the nonlinear problem.

2. ES - FG POROUS CYLINDRICAL SHELLS IN THERMAL ENVIRONMENT

Consider a thin circular cylindrical shell as shown in Fig. 1, with mean radius R, thickness h and length L subjected to torsion load of intensity τ. Two butt-ends of shell are assumed to be only deformed in their planes and they still are circular. The middle surface of the shells is referred to the coordinates (x, θ, z), $y = R\theta$. The coordinate axis x is chosen in the generatrix direction of the shell, while the coordinate axes y and z respond to the circumferential and thickness directions, respectively. The shell is stiffened by closely spaced circular rings and longitudinal stringers attached to the inside of the shell skin. The stiffeners are made of functionally graded materials. The material properties are assumed varying continuously through the thickness direction of the shell.

Young module and thermal expansion coefficient of shell and inside FGM stiffener are expressed by

$$(E_{sh}, \alpha_{sh}) = \begin{cases} (E_c, \alpha_c) + (E_{mc}, \alpha_{mc})\left(\dfrac{2z + h_{FG} + h_{core}}{h_{FG}}\right)^k, & -\dfrac{h_{FG} + h_{core}}{2} < z < -\dfrac{h_{core}}{2} \\ (E_m, \alpha_m)\left[1 - e_0 \cos\left(\dfrac{\pi z}{h_{core}}\right)\right], & -\dfrac{h_{core}}{2} < z < \dfrac{h_{core}}{2} \\ (E_c, \alpha_c) + (E_{mc}, \alpha_{mc})\left(\dfrac{-2z + h_{FG} + h_{core}}{h_{FG}}\right)^k, & \dfrac{h_{core}}{2} < z < \dfrac{h_{FG} + h_{core}}{2} \end{cases} \tag{1}$$

$$E_s = E_c + E_{mc}\left(\frac{2z - h}{2h_s}\right)^{k_2}, \quad \frac{h}{2} \le z \le \frac{h}{2} + h_s, \quad k_2 \ge 0, \tag{2}$$

$$E_r = E_c + E_{mc}\left(\frac{2z-h}{2h_r}\right)^{k_3}, \quad \frac{h}{2} \le z \le \frac{h}{2} + h_r, \quad k_3 \ge 0, \tag{3}$$
$$h = h_{FG} + h_{core}, \quad k \ge 0, \quad E_{mc} = E_m - E_c,$$

where e_0 is the porosity coefficient ($0 \le e_0 < 1$); $\alpha_{sh}, \alpha_m, \alpha_c$ - Thermal expansion coefficient of the shell, metal and ceramic, respectively.

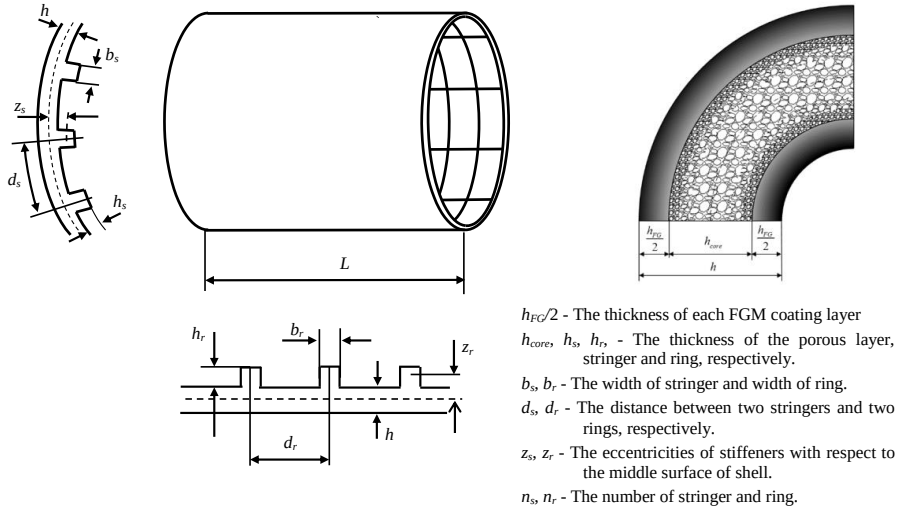

Fig. 1. Stiffened porous circular cylindrical shell with FG coating

According to [9], the Poisson's ratios are assumed to be constant $\nu_{sh} = \nu_s = \nu_r = \nu =$ const. k, k_2 and k_3 are the volume fractions indexes of shell, stringer and ring, respectively. The subscripts m, c, sh, s and r - denoting metal, ceramic, shell, stringers and ring, respectively. It is evident that, from Eqs. (1)–(3), a continuity between the shell and stiffeners is satisfied. Note that the thickness of the stringer and the ring are respectively denoted by h_s, and h_r; and E_c, E_m are Young's modulus of the ceramic and metal; and α_c, α_m are thermal expansion coefficient of ceramic and metal, respectively.

3. FUNDAMENTAL EQUATIONS AND SOLUTION OF THE PROBLEM

The nonlinear equilibrium equations of cylindrical shell, taking into account an elastic foundation, based on the first order shear deformation theory are given by [6, 15]

$$N_{x,x} + N_{xy,y} = 0,$$
$$N_{xy,x} + N_{y,y} = 0,$$
$$Q_{x,x} + Q_{y,y} + \frac{N_y}{R} + N_x w_{,xx} + 2N_{xy} w_{,xy} + N_y w_{,yy} + 2N_{xy}^0 w_{,xy} - K_1 w + K_2\left(w_{,xx} + w_{,yy}\right) = 0,$$

$$\frac{\partial M_x}{\partial x}+\frac{\partial M_{xy}}{\partial y}-Q_x=0,$$
$$\frac{\partial M_{xy}}{\partial x}+\frac{\partial M_y}{\partial y}-Q_y=0, \tag{4}$$

where K_1 (N/m^3) is modulus of subgrade reaction and K_2 (N/m) is the shear modulus of the subgrade.

Substituting the stress-strains N_{ij} and moments M_{ij} through the displacements u, v, w and slope rotation ϕ_x, ϕ_y into Eqs. (4), we obtain the following equation

$$C_{11}\left(u_{,xx}+w_{,x}w_{,xx}\right)+C_{12}\left(v_{,xy}-\frac{w_{,x}}{R}+w_{,y}w_{,xy}\right)+C_{14}\phi_{x,xx}+C_{15}\phi_{y,xy}$$
$$+C_{33}\left(u_{,yy}+v_{,xy}+w_{,xy}w_{,y}+w_{,x}w_{,yy}\right)+C_{36}\frac{1}{2}\left(\phi_{x,yy}+\phi_{y,xy}\right)=0, \tag{5}$$

$$C_{33}\left(u_{,xy}+v_{,xx}+w_{,xx}w_{,y}+w_{,x}w_{,xy}\right)+C_{36}\frac{1}{2}\left(\phi_{x,xy}+\phi_{y,xx}\right)$$
$$+C_{12}\left(u_{,xy}+w_{,x}w_{,xy}\right)+C_{22}\left(v_{,yy}-\frac{w_{,y}}{R}+w_{,y}w_{,yy}\right)+C_{24}\phi_{x,xy}+C_{25}\phi_{y,yy}=0, \tag{6}$$

$$C_7\left(w_{,xx}+\phi_{x,x}\right)+C_8\left(w_{,yy}+\phi_{y,y}\right)$$
$$+\frac{1}{R}\left[C_{12}\left(u_{,x}+\frac{1}{2}w_{,x}^2\right)+C_{22}\left(v_{,y}-\frac{w}{R}+\frac{1}{2}w_{,y}^2\right)+C_{24}\phi_{x,x}+C_{25}\phi_{y,y}-\phi_1-\phi_{1y}^T\right]$$
$$+\left[C_{11}\left(u_{,x}+\frac{1}{2}w_{,x}^2\right)+C_{12}\left(v_{,y}-\frac{w}{R}+\frac{1}{2}w_{,y}^2\right)+C_{14}\phi_{x,x}+C_{15}\phi_{y,y}-\phi_1-\phi_{1x}^T\right]w_{,xx}$$
$$+2\left[C_{33}\left(u_{,y}+v_{,x}+w_{,x}w_{,y}\right)+C_{36}\frac{1}{2}\left(\phi_{x,y}+\phi_{y,x}\right)\right]w_{,xy}$$
$$+\left[C_{12}\left(u_{,x}+\frac{1}{2}w_{,x}^2\right)+C_{22}\left(v_{,y}-\frac{w}{R}+\frac{1}{2}w_{,y}^2\right)+C_{24}\phi_{x,x}+C_{25}\phi_{y,y}-\phi_1-\phi_{1y}^T,\right]w_{,yy}$$
$$+2N_{xy}^0w_{,xy}x-K_1w+K_2\left(w_{,xx}+w_{,yy}\right)=0, \tag{7}$$

$$C_{14}\left(u_{,xx}+w_{,x}w_{,xx}\right)+C_{24}\left(v_{,xy}-\frac{w_{,x}}{R}+w_{,y}w_{,xy}\right)+C_{44}\phi_{x,xx}+C_{45}\phi_{y,xy}$$
$$+C_{63}\left(u_{,yy}+v_{,xy}+w_{,xy}w_{,y}+w_{,x}w_{,yy}\right)+C_{66}\frac{1}{2}\left(\phi_{x,yy}+\phi_{y,xy}\right)-C_7\left(w_{,x}+\phi_x\right)=0, \tag{8}$$

$$C_{63}\left(u_{,xy}+v_{,xx}+w_{,xx}w_{,y}+w_{,x}w_{,xy}\right)+C_{66}\frac{1}{2}\left(\phi_{x,xy}+\phi_{y,xx}\right)+C_{15}\left(u_{,xy}+w_{,x}w_{,xy}\right)$$
$$+C_{25}\left(v_{,yy}-\frac{w_{,y}}{R}+w_{,y}w_{,yy}\right)+C_{45}\phi_{x,xy}+C_{55}\phi_{y,yy}-C_8\left(w_{,y}+\phi_y\right)=0, \tag{9}$$

where the stiffness parameters C_{ij} and thermal parameters $\phi_1, \phi_2, \phi_{ij}^T$ can be found in Ref. [9] and

$$C_7=\frac{5}{6}\left[\int_{-h/2}^{h/2}\frac{E_{sh}}{2\left(1+\nu\right)}dz+\frac{b_s}{d_s}\int_{h/2}^{h/2+h_s}\frac{E_s\left(z\right)}{2\left(1+\nu\right)}dz\right],$$

$$C_8 = \frac{5}{6}\left[\int_{-h/2}^{h/2} \frac{E_{sh}}{2(1+\nu)}dz + \frac{b_r}{d_r}\int_{h/2}^{h/2+h_s} \frac{E_r(z)}{2(1+\nu)}dz\right].$$

Eqs. (5)–(9) are the nonlinear governing equations used to investigate the nonlinear buckling and postbuckling behavior of eccentrically stiffened FG porous cylindrical shells surrounded by elastic foundations and under uniform torsion loads in thermal environment based on first order shear deformation theory.

Assume that a torsion-loaded cylindrical shell surrounded by elastic foundations in thermal environment and it is simply supported at two butt-ends $x = 0$ and $x = L$. In this case, the deflection of shell is expressed by [16]

$$\begin{aligned} &u = U\sin\left(\frac{m\pi x}{L} + \frac{ny}{R}\right), \quad v = V\sin\left(\frac{m\pi x}{L} + \frac{ny}{R}\right), \quad w = W\cos\left(\frac{m\pi x}{L} + \frac{ny}{R}\right), \\ &\phi_x = \Phi_x\sin\left(\frac{m\pi x}{L} + \frac{ny}{R}\right), \quad \phi_y = \Phi_y\sin\left(\frac{m\pi x}{L} + \frac{ny}{R}\right), \end{aligned} \tag{10}$$

in which m is the number of axis half waves and n is the number of circumferential waves. It is found that the simply supported boundary condition at $x = 0$ and $x = L$ is fulfilled on the average sense.

Introduction of Eq. (10) into Eqs. (5)–(9), then applying Galerkin method in the ranges $0 \le y \le 2\pi R$ and $0 \le x \le L$, lead to

$$a_{11}U + a_{12}V + a_{13}W + a_{14}\Phi_x + a_{15}\Phi_y = 0, \tag{11}$$

$$a_{21}U + a_{22}V + a_{23}W + a_{24}\Phi_x + a_{25}\Phi_y = 0, \tag{12}$$

$$\begin{aligned} a_{31}U + a_{32}V + \Bigg[a_{33} + \left(\phi_1 + \phi_{1x}^T\right)\frac{m^2\pi^2}{L^2} + \left(\phi_1 + \phi_{1y}^T\right)\frac{n^2}{R^2} - 2N_{xy}^0\frac{mn\pi}{LR} \\ - K_1 - K_2\left(\frac{m^2\pi^2}{L^2} + \frac{n^2}{R^2}\right)\Bigg]W + a_{34}\Phi_x + a_{35}\Phi_y + a_{36}W^3 = 0, \end{aligned} \tag{13}$$

$$a_{41}U + a_{42}V + a_{43}W + a_{44}\Phi_x + a_{45}\Phi_y = 0, \tag{14}$$

$$a_{51}U + a_{52}V + a_{53}W + a_{54}\Phi_x + a_{55}\Phi_y = 0. \tag{15}$$

Using Eqs. (11), (12), (14) and (15) leads to

$$\frac{D_1}{D}W, \quad V = \frac{D_2}{D}W, \quad \Phi_x = \frac{D_3}{D}W, \quad \Phi_y = \frac{D_4}{D}W. \tag{16}$$

where the coefficients a_{ij}, D, D_i are given in Ref. [6].

Substituting Eqs. (16) into Eq. (13), taking into account $N_{xy}^0 = -\tau h$ obtains

$$-\frac{LR}{2mn\pi h}\begin{bmatrix} a_{31}\dfrac{D_1}{D} + a_{32}\dfrac{D_2}{D} + a_{33} + \left(\phi_1 + \phi_{1x}^T\right)\dfrac{m^2\pi^2}{L^2} + \left(\phi_1 + \phi_{1y}^T\right)\dfrac{n^2}{R^2} \\ -K_1 - K_2\left(\dfrac{m^2\pi^2}{L^2} + \dfrac{n^2}{R^2}\right) + a_{34}\dfrac{D_3}{D} + a_{35}\dfrac{D_4}{D} + a_{36}W^2 \end{bmatrix}. \quad (17)$$

Based on Eq. (17), the nonlinear buckling and post-buckling of ES-FGM cylindrical shell surrounded by elastic foundations and in thermal environment are analyzed.

Taking $W \to 0$, Eq. (17) leads to

$$\tau_{cr} = -\frac{LR}{2mn\pi h}\begin{bmatrix} a_{31}\dfrac{D_1}{D} + a_{32}\dfrac{D_2}{D} + a_{33} + \left(\phi_1 + \phi_{1x}^T\right)\dfrac{m^2\pi^2}{L^2} + \left(\phi_1 + \phi_{1y}^T\right)\dfrac{n^2}{R^2} \\ -K_1 - K_2\left(\dfrac{m^2\pi^2}{L^2} + \dfrac{n^2}{R^2}\right) + a_{34}\dfrac{D_3}{D} + a_{35}\dfrac{D_4}{D} \end{bmatrix}. \quad (18)$$

Eq. (18) is used to find critical loads of eccentrically stiffened cylindrical shells surrounded by elastic foundations in thermal environment based on the first order shear deformation theory.

4. NUMERICAL RESULTS

4.1. Comparative results

In order to demonstrate the accuracy of the present approach, the comparisons on critical torsion load are made with results from open literatures.

Basing on Eq. (18), the buckling load is determined by minimization critical load with respect to m and n. Table 1 compares the results of this paper for stiffened cylindrical shell under torsion load with the results given in reference [6]. It can be seen from Table 1 that good agreements between the present results and the reference results are taken.

Table 1. Comparison of critical torsion loads of stiffened cylindrical shell for h = 0.005 m, R/h = 50, L/R = 2, $h_s = h_r$ = 0.005 m, $b_s = b_r$ = 0.005 m, $K_1 = 1.5 \times 10^7$ N/m^3, $K_2 = 1.5 \times 10^5$ N/m, $\Delta T = 0^\circ$C

τ (MPa)	Stringer (n_s = 40, n_r = 0)		Ring (n_s = 0, n_r = 40)		Orthogonal ($n_s = n_r$ = 20)	
	Ref. [6]	Present by Eq. (18)	Ref. [6]	Present by Eq. (18)	Ref. [6]	Present by Eq. (18)
Ceramic	929.44766 (1, 5)*	929.448 (1, 5)	2056.14803 (1, 4)	2056.148 (1, 4)	1602.16579 (1, 4)	1602.166 (1, 4)
Metal	223.74721 (1, 5)	223.747 (1, 5)	426.90258 (1, 4)	426.903 (1, 4)	343.27428 (1, 4)	343.274 (1, 4)

*buckling modes (m, n).

In the following subsections, a cylindrical shell FG face/Metal foam core/FG face reinforced by stiffeners surrounded by Pasternak elastic foundations is considered. The functionally graded materials of face sheets and stiffeners are mixture of Alumina with $E_c = 380$ GPa, $\alpha_c = 5.4 \times 10^{-6}$ K^{-1} and Aluminum with $E_m = 70$ GPa, $\alpha_m = 22.2 \times 10^{-6}$ K^{-1} and Poisson ratio $\nu = 0.3$. The geometrical and elastic foundation parameters are taken as: $k_2 = k_3 = k = 1$, $h = 0.006$ m, $L/R = 1.5$, $R/h = 70$, $h_{core}/h_{FG} = 3$, $e_0 = 0.6$, $\Delta T = 0$ K, $h_s = h_r = 0.006$ m, $b_s = b_r = 0.006$ m, $n_s = 18$, $n_r = 18$, $K_1 = 4 \times 10^7$ N/m^3, $K_2 = 3 \times 10^5$ N/m. This is the database and in each sub-section, when investigating the effect of a certain parameters, that value is varied.

4.2. Effect of e_0 and h_{core}/h_{FG}

Basing on Eq. (18), the buckling load is determined by minimization critical load with respect to m and n. Table 2 describes the effect of porosity coefficient and core layer on the buckling load. It shows that the critical load decrease when the porosity coefficient increases. This point is also presented in Figs. 2 and 3 when using Eq. (17), illustration the load-deflection curves and the buckling load-porosity coefficient e_0 curves of ES porous cylindrical sandwich shell. It indicates that the loading capacity of the sandwich cylindrical shell is decreased when e_0 is increased. In fact, according to Eqs. (1), the porosity significantly affect Young modulus of porous shells.

With the total thickness constant, Table 2 presents the critical buckling loads of ES porous cylindrical sandwich shell for different thickness of core layer-to-FG face layer ratio h_{core}/h_{FG} corresponding to the buckling mode. Fig. 4 also illustrate the effect of h_{core}/h_{FG} ratio on the load-deflection curves of porous sandwich shell. It can be seen that when h_{core}/h_{FG} increases, the critical buckling loads decrease. When illustration the load-deflection curves and buckling load-thickness ratio h_{core}/h_{FG} curves of ES porous cylindrical sandwich shell, this point is also presented in Figs. 4 and 5.

Table 2. Effect of porosity coefficients e_0 and core layer h_{core}/h_{FG} on critical load $k_2 = k_3 = k = 1, h = 0.006$ m, $L/R = 1.5, R/h = 70, h_{core}/h_{FG} = 3, e_0 = 0.6, \Delta T = 0$ K, $h_s = h_r = 0.0064$ m, $b_s = b_r = 0.006$ m, $n_s = 18$, $n_r = 18$, $K_1 = 4 \times 10^7$ N/m^3, $K_2 = 3 \times 10^5$ N/m

τ (MPa)	$e_0 = 0$	$e_0 = 0.2$	$e_0 = 0.4$	$e_0 = 0.6$	$e_0 = 0.8$
$h_{core}/h_{FG} = 0$	789.871 (1, 5)*	789.871 (1, 5)	789.871 (1, 5)	789.871 (1, 5)	789.871 (1, 5)
$h_{core}/h_{FG} = 1$	642.683 (1, 5)	636.408 (1, 5)	630.079 (1, 5)	623.694 (1, 5)	617.247 (1, 5)
$h_{core}/h_{FG} = 3$	539.022 (1, 5)	527.710 (1, 5)	516.144 (1, 5)	504.282 (1, 5)	492.078 (1, 5)
$h_{core}/h_{FG} = 5$	497.934 (1, 5)	484.333 (1, 5)	470.304 (1, 5)	455.763 (1, 5)	440.602 (1, 5)
$h_{core}/h_{FG} = \infty$	402.192 (2, 6)	373.734 (2, 6)	344.486 (2, 6)	314.188 (2, 6)	282.448 (2, 6)

*buckling modes (m, n).

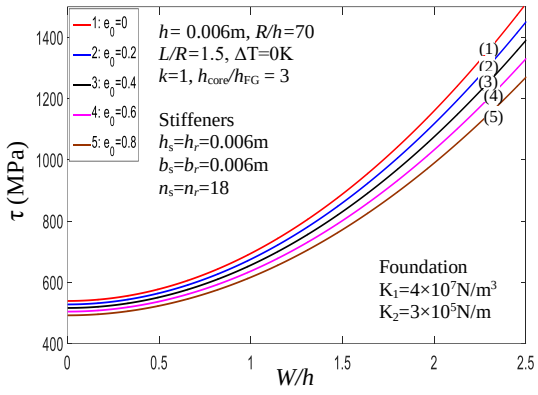

Fig. 2. Effects of e_0 on postbuckling behavior

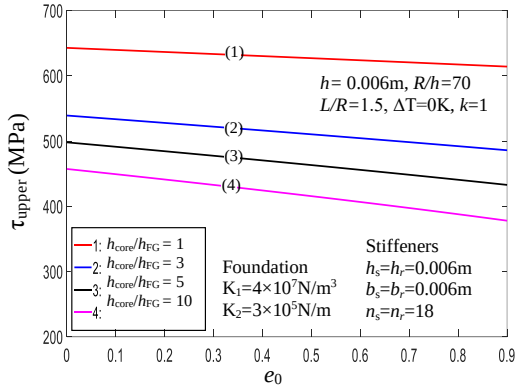

Fig. 3. Effects of e_0 on upper torsional load τ_{upper}

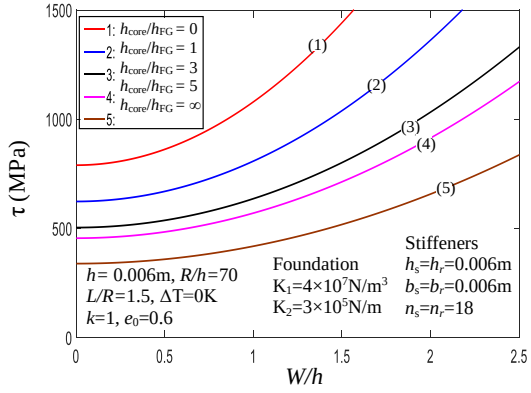

Fig. 4. Effects of h_{core}/h_{FG} on postbuckling behavior

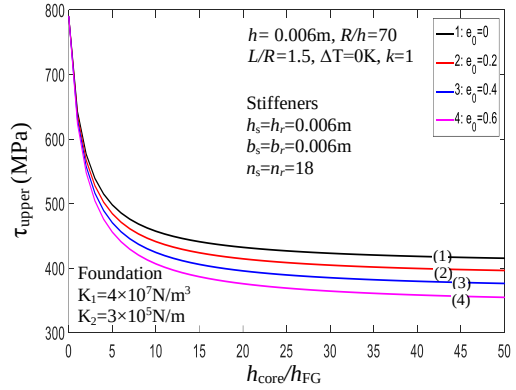

Fig. 5. Effects of h_{core}/h_{FG} on upper torsional load

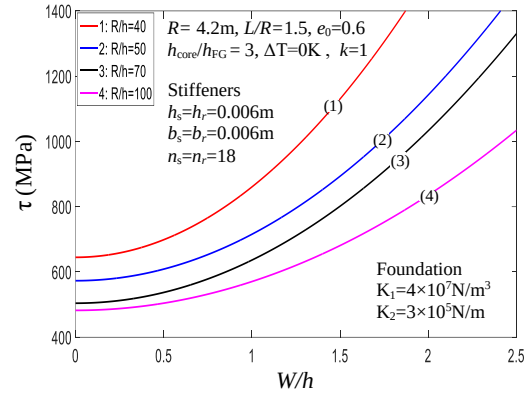

Fig. 6. Effects of R/h on postbuckling behavior

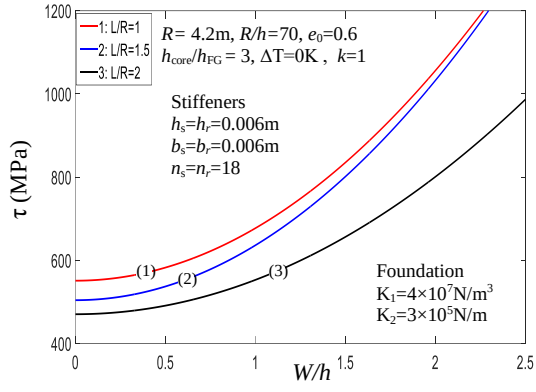

Fig. 7. Effects of L/R on postbuckling behavior

4.3. Effect of R/h and L/R ratios

Table 3 and Figs. 6 and 7 present effects of R/h and L/R ratios on critical load and postbuckling behavior. It is observed that the buckling load τ decreases markedly with the increase of R/h ratio, i.e. the more the shell is thin the more the value of critical load is small. As can be observed, the capacity of mechanical load q bearing of the FGP shells is considerably reduced with the increase of L/R.

Table 3. Effect of R/h and L/R on critical load $k_2 = k_3 = k = 1, R = 0.42$ m, $L/R = 1.5, R/h = 70, h_{core}/h_{FG} = 3, e_0 = 0.6, \Delta T = 0$ K, $h_s = h_r = 0.006$ m, $b_s = b_r = 0.006$ m, $n_s = 18, n_r = 18, K_1 = \times 10^7$ N/m^3, $K_2 = 3 \times 10^5$ N/m

τ (MPa)	$L/R = 1$	$L/R = 1.5$	$L/R = 2$	$L/R = 3$
$R/h = 30$	1055.686 (1, 4)*	818.678 (1, 4)	766.512 (1, 4)	608.513 (1, 3)
$R/h = 40$	787.764 (1, 5)	644.903 (1, 4)	581.546 (1, 4)	525.765 (1, 3)
$R/h = 50$	654.884 (1, 5)	573.198 (1, 4)	507.723 (1, 4)	508.425 (1, 3)
$R/h = 70$	551.133 (1, 5)	504.282 (1, 5)	470.548 (1, 4)	438.078 (2, 5)
$R/h = 100$	521.547 (1, 5)	482.359 (2, 6)	453.152 (2, 6)	418.706 (3, 6)

*buckling modes (m, n).

4.4. Effect of volume fraction index, temperature and stiffeners

The effects of volume fraction index on the critical buckling load of FGP shell are considered in Table 4, Figs. 8, 10 and 11. It is found that, the critical buckling load decreases with the increase of k. This property is suitable to the real property of material, because the higher value of k corresponds to a metal-richer shell which usually has less stiffness than a ceramic-richer one.

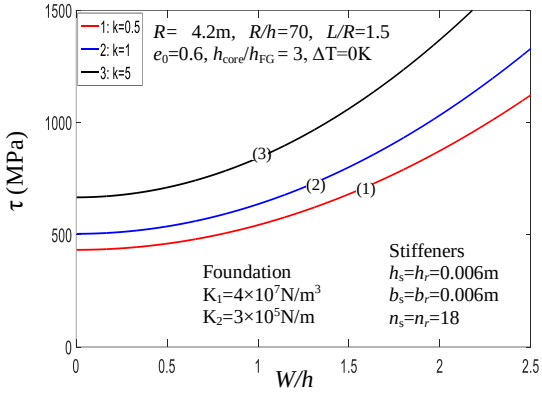

Fig. 8. Effects of k on postbuckling behavior

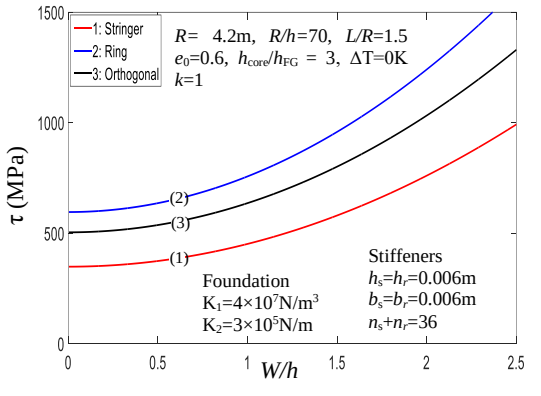

Fig. 9. Effects of stiffeners on postbuckling behavior

Table 4. Effect of a/b and a/R on critical load $k_2 = k_3 = k, h = 0.006$ m, $L/R = 1.5$, $R/h = 70, h_{core}/h_{FG} = 3, e_0 = 0.6, \Delta T = 0$ K, $h_s = h_r = 0.006$ m, $b_s = b_r = 0.006$ m, $n_s = 18, n_r = 18, K_1 = 4 \times 10^7$ N/m^3, $K_2 = 3 \times 10^5$ N/m

τ (MPa)		Stringer $n_s = 36, n_r = 0$	Ring $n_s = 0, n_r = 36$	Orthogonal $n_s = n_r = 18$
$\Delta T = 0$ K	Metal	226.626 (2, 7)*	333.925 (2, 6)	299.116 (1, 5)
	$k = 0.5$	310.045 (1, 5)	498.616 (1, 4)	432.902 (1, 5)
	$k = 1$	348.847 (1, 5)	573.007 (1, 4)	504.282 (1, 5)
	$k = 5$	421.456 (1,5)	737.735 (1,4)	666.828 (1,5)
	Ceramic	453.887 (1,5)	837.984 (1,4)	756.674 (1,4)
$\Delta T = 50$ K	Metal	138.615 (1, 6)	239.695 (1, 5)	205.528 (1, 5)
	$k = 0.5$	201.641 (1, 6)	352.552 (1, 5)	302.385 (1, 5)
	$k = 1$	241.549 (1, 5)	436.383 (1, 5)	370.801 (1, 5)
	$k = 5$	322.125 (1, 5)	614.662 (1, 4)	544.327 (1, 5)
	Ceramic	362.628 (1, 5)	726.781 (1, 4)	658.412 (1, 5)

*buckling modes (m, n).

The effect of uniform temperature rise on the buckling and postbuckling is considered in this subsection. Table 4 shows the effect of temperature on these upper and lower loads. The effects of temperature on buckling load are also shown in Fig. 11. It can be seen that the upper torsional load of shell reduces when ΔT increases.

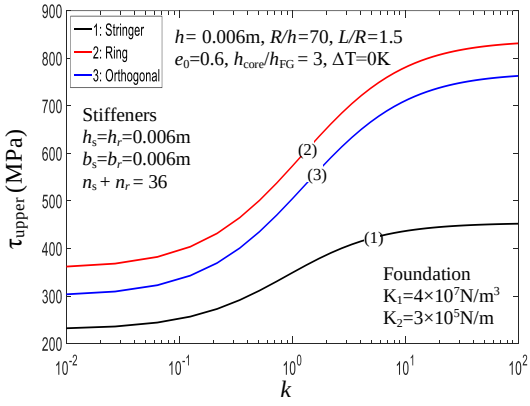

Fig. 10. Effects of stiffeners and k on upper torsional load τ_{upper}

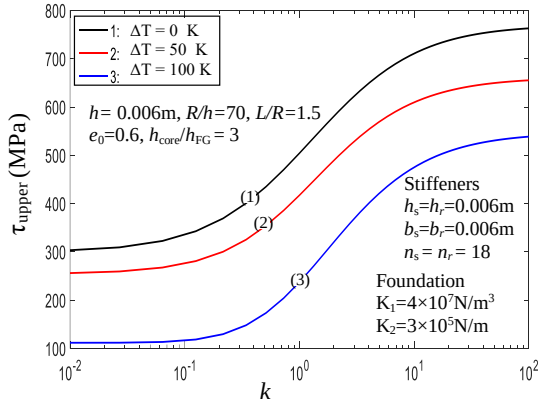

Fig. 11. Effects of ΔT and k on upper torsional load τ_{upper}

The effects of stiffeners on critical loads are given in Table 4, Figs. 9 and 10. As can be seen that, the critical load of FGP shell reinforced by stringers is the smallest, the critical load of FGP cylindrical shell reinforced by rings is biggest.

5. CONCLUSIONS

An analytical approach to analyze the nonlinear buckling and post-buckling behavior of eccentrically stiffened functionally graded porous cylindrical shells under torsional load and surrounded by elastic foundations based on the first order shear deformation theory and the smeared stiffeners technique with geometrical nonlinearity in von Kármán sense is presented in this paper. The shell is reinforced by eccentrically rings and stringers attached to the inside and material properties of shell and stiffeners varying continuously graded in the thickness direction are considered.

The results obtained show that foundation and stiffener enhance strongly on the stability and load-carrying capacity of FGP cylindrical shells. The study also shows the pronounced effects of porosity coefficient, the thickness of the porous core layer and thermal element on the critical buckling loads and postbuckling load-deflection curves.

DECLARATION OF COMPETING INTEREST

The authors declare that they have no known competing financial interests or personal relationships that could have appeared to influence the work reported in this paper.

FUNDING

This research received no specific grant from any funding agency in the public, commercial, or not-for-profit sectors.

REFERENCES

[1] H.-S. Shen. Torsional buckling and postbuckling of FGM cylindrical shells in thermal environments. *International Journal of Non-Linear Mechanics*, **44**, (2009), pp. 644–657. https://doi.org/10.1016/j.ijnonlinmec.2009.02.009.

[2] H. Huang and Q. Han. Nonlinear buckling of torsion-loaded functionally graded cylindrical shells in thermal environment. *European Journal of Mechanics - A/Solids*, **29**, (2010), pp. 42–48. https://doi.org/10.1016/j.euromechsol.2009.06.002.

[3] P. Zhang and Y. Fu. Torsional buckling of elastic cylinders with hard coatings. *Acta Mechanica*, **220**, (2011), pp. 275–287. https://doi.org/10.1007/s00707-011-0482-2.

[4] R. C. Batra. Torsion of a functionally graded cylinder. *AIAA Journal*, **44**, (2006), pp. 1363–1365. https://doi.org/10.2514/1.19555.

[5] D. V. Dung and L. K. Hoa. Nonlinear torsional buckling and postbuckling of eccentrically stiffened FGM cylindrical shells in thermal environment. *Composites Part B: Engineering*, **69**, (2015), pp. 378–388. https://doi.org/10.1016/j.compositesb.2014.10.018.

[6] L. K. Hoa and D. V. Dung. Nonlinear torsional buckling and postbuckling of FGM cylindrical shells reinforced by FGM stiffeners in thermal environment using FSDT in terms of displacement components. In *Proceeding of the 12th National Conference on Deformable Solid Mechanics*, (2015), pp. 583–590.

[7] P. T. Thang, N. D. Duc, and T. Nguyen-Thoi. Thermomechanical buckling and post-buckling of cylindrical shell with functionally graded coatings and reinforced by stringers. *Aerospace Science and Technology*, **66**, (2017), pp. 392–401. https://doi.org/10.1016/j.ast.2017.03.023.

[8] D. G. Ninh and D. H. Bich. Nonlinear torsional buckling and post-buckling of eccentrically stiffened ceramic functionally graded material metal layer cylindrical shell surrounded by elastic foundation subjected to thermo-mechanical load. *Journal of Sandwich Structures & Materials*, **18**, (2016), pp. 712–738. https://doi.org/10.1177/1099636216644787.

[9] V. H. Nam, N.-T. Trung, and L. K. Hoa. Buckling and postbuckling of porous cylindrical shells with functionally graded composite coating under torsion in thermal environment. *Thin-Walled Structures*, **144**, (2019). https://doi.org/10.1016/j.tws.2019.106253.

[10] K. Foroutan, A. Shaterzadeh, and H. Ahmadi. Nonlinear static and dynamic hygrothermal buckling analysis of imperfect functionally graded porous cylindrical shells. *Applied Mathematical Modelling*, **77**, (2020), pp. 539–553. https://doi.org/10.1016/j.apm.2019.07.062.

[11] H. Ahmadi and K. Foroutan. Nonlinear static and dynamic thermal buckling analysis of imperfect multilayer FG cylindrical shells with an FG porous core resting on nonlinear elastic foundation. *Journal of Thermal Stresses*, **43**, (2020), pp. 629–649. https://doi.org/10.1080/01495739.2020.1727802.

[12] K. Foroutan and H. Ahmadi. Nonlinear static and dynamic buckling analyses of imperfect FGP cylindrical shells resting on nonlinear elastic foundation under axial compression. *International Journal of Structural Stability and Dynamics*, **20**, (2020). https://doi.org/10.1142/s0219455420500741.

[13] D. Shahgholian-Ghahfarokhi, G. Rahimi, A. Khodadadi, H. Salehipour, and M. Afrand. Buckling analyses of FG porous nanocomposite cylindrical shells with graphene platelet reinforcement subjected to uniform external lateral pressure. *Mechanics Based Design of Structures and Machines*, **49**, (2020), pp. 1059–1079. https://doi.org/10.1080/15397734.2019.1704777.

[14] D. Shahgholian, M. Safarpour, A. R. Rahimi, and A. Alibeigloo. Buckling analyses of functionally graded graphene-reinforced porous cylindrical shell using the Rayleigh–Ritz method. *Acta Mechanica*, **231**, (2020), pp. 1887–1902. https://doi.org/10.1007/s00707-020-02616-8.

[15] J. N. Reddy. *Mechanics of laminated composite plates and shells*. CRC Press, (2003). https://doi.org/10.1201/b12409.

[16] A. Takano. Buckling of thin and moderately thick anisotropic cylinders under combined torsion and axial compression. *Thin-Walled Structures*, **49**, (2011), pp. 304–316. https://doi.org/10.1016/j.tws.2010.11.001.